Optics and Photonics Journal, **2012, 2, 73-84**
http://dx.doi.org/10.4236/opj.2012.22011 Published Online June 2012 (http://www.SciRP.org/journal/opj)

Effect of Experimental Parameters on the Fabrication of Gold Nanoparticles via Laser Ablation

Hisham Imam[1], Khaled Elsayed[2], Mohamed A. Ahmed[2], Rania Ramdan[2]
[1]National Institute of Laser Enhanced Sciences, Cairo University, Giza, Egypt
[2]Materials Science Laboratory (1), Physics Department, Faculty of Science, Cairo University, Giza, Egypt
Email: hishamimam@niles.edu.eg

Received April 9, 2012; revised May 12, 2012; accepted May 22, 2012

ABSTRACT

In this study we report the effect of laser parameters such as laser energy, laser wavelength as well as focusing condition of laser beam on the size and morphology of the gold nanoparticles (GNPs) prepared in deionised water by pulsed laser ablation. The optimum conditions at which gold nanoparticles obtained with controllable average size have been reported as these parameters affected the size, distribution and absorbance spectrum. Effect of energy was studied. The laser energy was divided into three regions (low, middle and high). A noteworthy change was observed at each region, as the average size changed from 5.9 nm at low energy to 14.4 nm at high energy and the gold nanoparticles reached a critical size of 8 nm at 100 mJ. The Effect of the wavelength on the particle size was examined at 1064 nm, 532 nm. It was found that, the optimum ablation laser wavelength was 1064 nm. Finally, significant results obtained when the effect of focusing conditions studied.

Keywords: Laser Ablation; Goldnanparticle

1. Introduction

In the last few years and due to unique physicochemical characteristics of gold nanoparticles and their wide usages in different fields, the number of publications on the preparation and characterization of gold nanoparticles has extensively increased [1,2]. For example, the recently recognized behavior of gold to act as a soft Lewis acid and large surface-to-volume ratio of nanogold as well as its inert property have widely enhanced the application of gold nanoparticles as a catalyst in the field of organic synthesis [1]. The ability of gold to produce heat after absorbing light provides a medicinal usage named as photothermal therapy [3]. All mentioned usages together with application of nanogold in gene and drug delivery increased studies on development of methods for gold nanoparticles production [4,5]. Although preparation of nanogold by physical procedures (such as laser ablation) provides gold nanoparticles with narrow range of particle size, it needs expensive equipments and has low yield [6]. Hazardous effects of organic solvents, reducing agents and toxic reagents applied for synthesis of gold nanoparticles on environment, encouraged researchers to developeco-friendly methods for preparation of gold nanoparticles [7,8].

Also due to their size-dependent physical and chemical properties [9-11], gold nanoparticles have optical, electrical, magnetic and mechanical properties which make them suitable for many applications such as drug and gene delivery [12,13], the ability to generate table immobilization of biomolecules [14] and in several targeting application [15]. There are several methods for preparing metal nanoparticles such as pulsed laser deposition [16], flame metal combustion [17], chemical reduction [18], photo-reduction [19], electrochemical reduction [20], solvothermal [21], electrolysis [22], green method [23], microwave induced [24], sonoelectrochemical [25], aerosol flow reactor [26], photochemical reduction [27], chemical fluid deposition [28], spray pyrolysis [29,30], and spark discharge [31]. Among them, the pulsed laser ablation in liquids PLAL has become an increasingly popular top-down approach [32] for producing nanoparticles. It's a relatively new method that was first introduced by Fojtik *et al*. in 1993 [33] as is a promising technique for the controlled fabrication of nanomaterials via rapid reactive quenching of ablated species at the interface between the plasma and liquid with high-quality nanoparticles free from chemical reagents. Therefore, PLAL process has received much attention as a novel NPs production technique. The most advanced method for producing nanostructured materials has been developed performing pulsed laser ablation of gold plate in liquids [34-38]. Advantages of this method include the relative simplicity of the procedure and the absence of chemical reagents in the final preparation, but the size distributions of the

GNPs prepared by this technique tend to be broadened due to the agglomeration and ejection of large fragments during laser ablation. To achieve the particlesize reduction, different surfactants can be used [39-41]. Another important advantages gold nanoparticles prepared by PLAL process were stable for a period of months. The main aim of the present study is to prepare pure gold nanoparticles in easy, fast and one step method via PLAL process in deionised water at various laser fluencies and wavelengths. The effect of the focusing conditions on the formation and fabrication of metal nanoparticles has not been approached by many researchers before. In this paper we discuss the focusing conditions that play an important role in the formation of small and narrowly dispersed gold nanoparticles and elucidate the mechanisms of the nanoparticles growth.

2. Experimental Setup

The formation of gold nanoparticles is fabricated via pulsed laser ablation of the corresponding gold metal plate (99.99%) of 3 mm thickness and its dimensions 1.5 × 1 cm^2 immersed into the liquid as shown in **Figure 1**. The gold plate was thoroughly washed with ethanol and deionised water to remove organic contamination and placed at the bottom of a glass vessel filled with 50 ml of an aqueous solution of deionized water. The gold metal plate was kept at 15 mm below the liquid surface. Pulsed Q-Switched laser Nd:YAG (Surelite II, Continuum) was used. The laser beam was operated at fundamental wavelength 1064 nm or second harmonic 532 nm and 10 Hz. The laser beam was focused by a plano-convex lens with focal length of 5 cm. The energy of the laser pulse was measured by power meter (OPHIR-NOVA). The ablation process was typically done for 5 minutes at room temperature. The laser beam was focused on the surface of the target and it was scanned over by using X-Y stage to avoid the craters on the surface of target. Morphology and size distribution of nanoparticles were characterized by HTEM (JEOL 1200). The solution containing GNPs was inserted in the bath of ultrasonicator for half of an hour and a drop of solution containing gold nanoparticles onto carbon coated copper grids and kept to completely dry at room temperature. The diameter of more than 100 nanoparticles in sight on a given micro graph was directly measured and the distribution of the particle diameters was obtained. The optical absorption spectrum of the solution was measured with UV-Vis spectrophotometer (PG instrument Ltd., T80+).

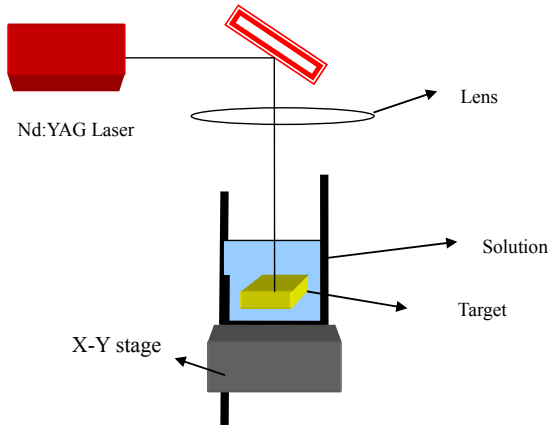

Figure 1. Schematic diagram of experimental setup.

3. Results and Discussion

3.1. Effect of Energy of Laser Beam

Laser energy was adjusted by inserting different glass sheets in the path of the laser beam before it reached the focus of the lens. In this section, the effect of laser fluence was studied on the obtained gold nanoparticles, their distribution and their optical spectrum. The energy of laser ranged between (10 - 250 mJ), which can be divided into three regions, low energy (10 mJ), middle region (20 - 100 mJ) and high energy (150 - 250 mJ). And there are three different laser ablation mechanisms in these three regions.

3.1.1. At Low Energy of Laser Beam (10 mJ)

Under the action of the laser at low energy the target is heated, but due to the strong confinement of the liquid at the surface, the vaporization rate is strongly restricted and no plume forms. In the absence of a vapor plume, the hot target is remained in contact with water promoting the oxidation of the nanoparticle oxides [42]. The reaction is initiated with the oxidation of the molten target surface by oxygen splitting of water molecules at the hot target so the hydroxide nanoparticles exist on the target surface. The gold hydroxide material on the surface then desorbs from the hot target surface and diffuses into the water and it isn't aggregated due to their negative charge so the average size of produced gold nanoparticles is small and they are produced by thermal vaporization as shown in **Figure 2**.

The average size is 5.9 nm and as it's shown the particles are small and have spherical shape and the yield is small and this is due to the negative charge on gold nanoparticles which prevents them from aggregation and their yield is small due to presence of water at the surface of the target which restricts their growing as explained above.

3.1.2. Intermediate Energy of Laser Beam (Plume Mixing Zone) (20 - 100 mJ)

In this stage the plume develops more slowly and is limited to a size much smaller than in a gas atmosphere [43]. The large pressure in the confined vapor plume

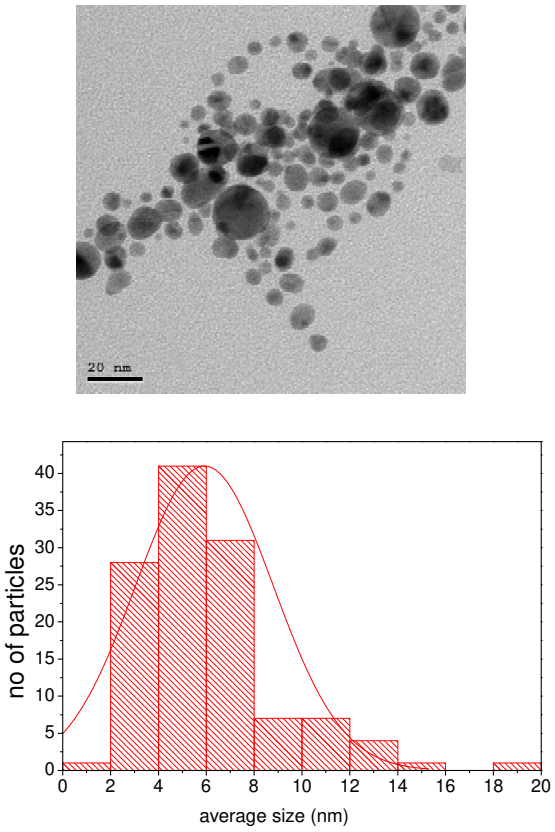

Figure 2. The TEM micrograph and histogram of gold nanoparticles prepared in 10 mJ.

results in an expansion beyond the equilibrium point, the internal plume pressure equals the hydrostatic pressure of the liquid, increasing the difference between the pressure inside and outside the plume decrease the expansion until it is stopped, the hydrostatic pressure then collapse, the plume back into the target. In this region, the nanoparticles fall into two distinct size distributions those are attributed to:

1) Target surface vaporization;

2) Explosive ejection of molten droplets directly from the target. And this leads to abroad size distribution as shown in **Figures 3(a)-(e)**.

The surface vaporization was discussed above, the explosive ejection occurs when the temperature approaches the thermodynamics critical temperature, thermal fluctuation is amplified and the rate of homogenous bubble nucleation rises dramatically and the target makes rapid transition from superheated liquid to a mixture of vapor and equilibrium liquid droplet. At this fluence, the momentum of a plume allows it to expand further out into the liquid, increasing the plasma life time and this results in an increase of screening of laser light from surface of bulk Gold target [44,45].

The data in the histograms show that, the average size of gold nanoparticles prepared in pure water at 20, 30, 40, 50, 100 mJ are 14.3, 13.2, 12.9, 12.2 and 8.08 respectively. As it is shown the average size decreases with the increasing of laser energy and from TEM micrographs it is found that, as laser energy increases, the particles become homogenous and have spherical shape and also the concentration increases until it reaches to their critical size at 100 mJ, and then the particles appear as diffused particles. The decrease in the average size of gold nanoparticles can be attributed to large energy which excited the gold nanoparticles in a solution, the photon energy is readily converted to the internal modes of the nanoparticles as during a single laser pulse, one gold nanoparticle is considered to absorb consecutively more than one thousand photon and it's temperature rises significantly so that the nanoparticle starts to fragment. After the single laser pulse the diffused into the solution and the temperature of nanoparticles return to room temperature before the next one arrive. The heating and cooling of nanoparticles occur in every laser pulse.

3.1.3. At High Energy of Laser Beam (Plasma Etching) (150 - 250 mJ)

At the high energy, laser energy is absorbed in the liquid to the target resulting material removal by reactive sputtering rather than direct laser ablation, as the intensity of laser in the presence of ablated material in the water, as this happen the amount of the light reaching to the target goes to zero, plasma formation in the water creates a cavitations bubble that expand and then collapse, driving highly energetic species into target [46]. In this region the average size of gold nanoparticles begins to increase again as shown in **Figures 4(a)-(c)**.

From the above figure, the average size of gold nanoparticles prepared in pure water at 150, 200 and 250 mJ are 11, 12.8 and 14.4 nm respectively it is observed that when laser energy exceed certain value (above 100 mJ) the average size and concentration begin to increase and the shape of prepared GNPs begins to take the spherical shape again after their shape was diffused when it prepared at 100 mJ this can be explained as when the GNPs reach their critical size, small fragments such as gold atoms and small aggregates resulting from photo fragmentation are dispersed in solution, therefore the nanoparticles present in the solution grow by attracting these small fragments. The fragmentation rate must increase with increasing the laser energy because the internal energy of irradiated nanoparticles increases. On the other hand, the aggregation rate increases with the increase of the concentration of the small fragments, after the laser is off, the fragmentation is terminated so that only the aggregation proceeds until the gold atoms and small fragments are consumed. The fragmentation rate of each nanoparticle decreases because it's absorption coefficient per atom decreases with it's diameter. In contrast

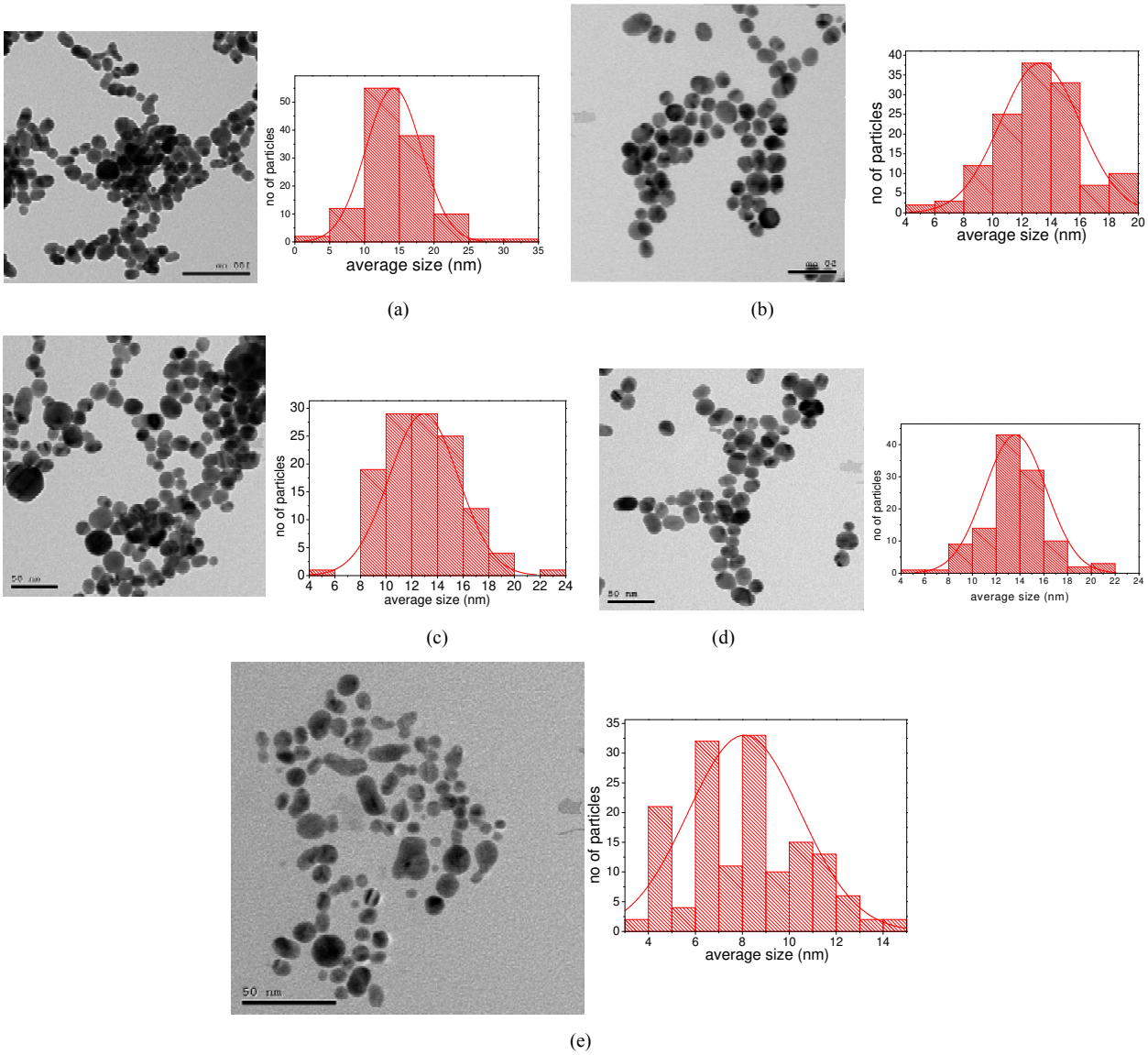

Figures 3. (a)-(e) TEM micrographs and their histograms of gold nanoparticles prepared in 20, 30, 40, 50, 100 mJ respectively.

the aggregation rate increases because the concentration of the small fragments increases, therefore, the minimum diameter is realized when the rate of fragmentation is equal to that of the aggregation [46]. From the above discussion, the average size decreases as the energy increases until it reach to the critical size then it begins to increases again as shown in the **Table 1** and **Figure 5**. The absorbance spectrum is studied which give indication on the concentration and size distribution of the gold nanoparticles prepared and this will ensure the results obtained from TEM as shown in **Figure 6**.

From the **Figure 6**, as the laser energy increases, the height of the Plasmon peak increases which indicate to the increase in the concentration of nanoparticles, till the nanoparticles reach it's critical size and the absorption coefficient of gold nanoparticles decreases and they couldn't absorb any more as they couldn't be fragment again, red shift in the Plasmon peak ensure the decrease in the average size of gold nanoparticles. As the laser energy increases, the Plasmon peak becomes narrower indicating that the particles have a homogenous distribution as the laser energy increases. The absorbance spectrum obtained at high laser energy is shown in **Figure 7**.

At high laser energy (150 - 250 mJ) as shown above, the absorbance shows an increase in the Plasmon peak with increasing the laser energy, indicating to the increase in the concentration of gold nanoparticles as the energy increase the peak becomes more narrow and there is a blue shift in Plasmon peak as the energy increase as the size of the gold nanoparticles increase. These results are matching as obtained from TEM.

So, the operating above or below the threshold will

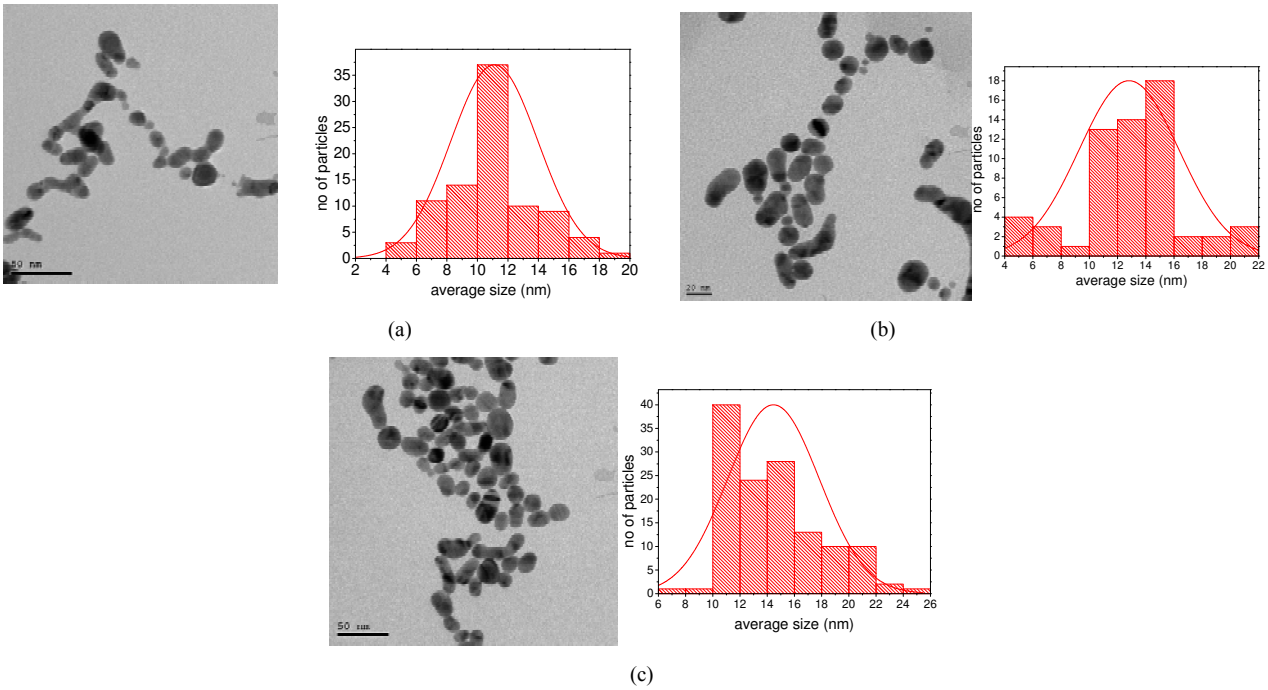

Figures 4. (a)-(c) TEM micrographs and histogram of gold nanoparticles prepared in pure water at 150, 200 and 250 mJ respectively.

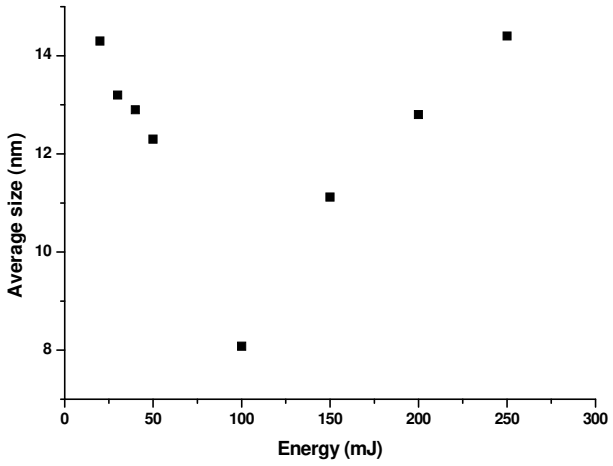

Figure 5. The relation between the energy and the average size.

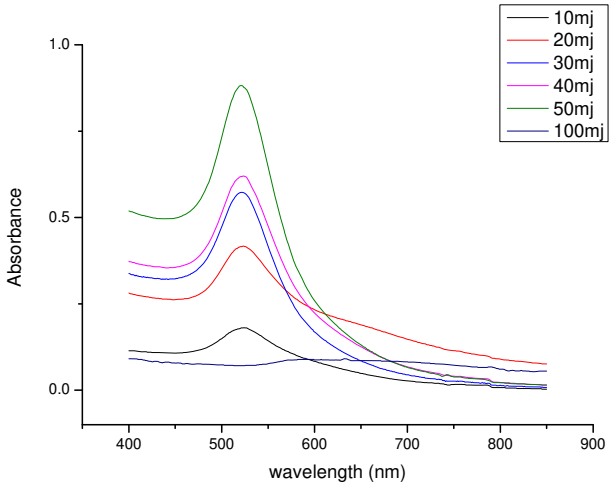

Figure 6. The absorbance spectrum of gold nanoparticles prepared in pure water at (10 - 100 mJ).

therefore allows the experimenter to choose between a low quality of small, narrowly distributed nanoparticles and much larger quantity but with a wider size distribution.

3.2. Effect of Wavelength

Effect of laser wavelength was examined at 1064 nm, 532 nm, the gold nanoparticles was fabricated using two laser beam at 1064 nm and 532 nm. From TEM as shown in **Figure 8** the particles distributions of 1064 are more homogenous and the average size of GNPs prepared at 532 nm is smaller than that prepared at 1064 nm.

The average size of GNPs prepared at 532 nm is 13.7 nm and 14.5 nm at 1064 mm. This can be contributed to two factors: The value of the absorption coefficient of bulk gold is higher at 532 nm, so the intensity of absorbance peak of 532 nm higher than 1064 nm. The photon energy of 532 nm is higher than that at 1064 nm, which lead to the fragmentation of GNPs prepared at 532 nm, the average size of GNPs prepared at 532 nm is smaller than that prepared at 1064 nm. in terms of the amount of ablated Au as determined by the area of surface Plasmon

Table 1. The relation between energy and average size of obtained gold nanoparticles.

Energy (mJ)	Average size(nm)
20	14.3
30	13.2
40	12.9
50	12.3
100	8.08
150	11.12
200	12.8
250	14.4

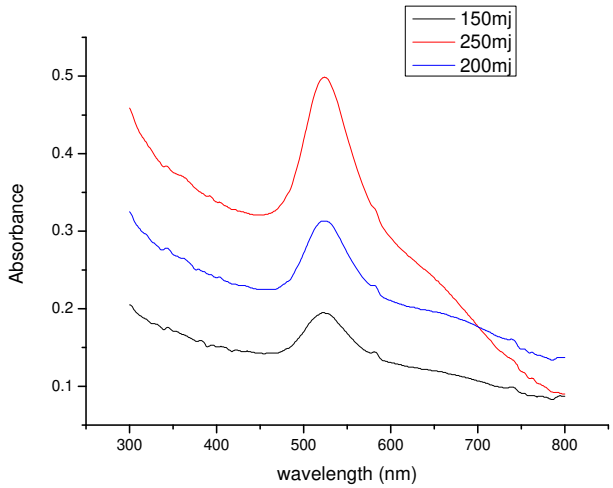

Figure 7. The absorbance spectrum of gold nanoparticles prepared in pure water at high laser fluence.

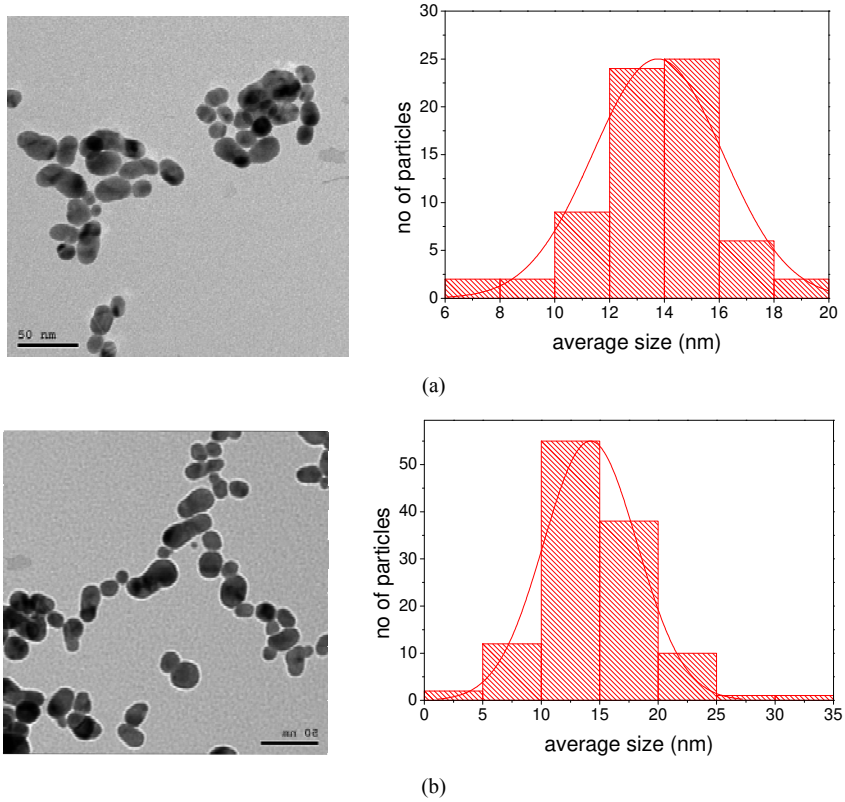

Figure 8. The TEM and histogram of GNPS prepared at 532 nm, 1064 nm respectively.

peak of the resulting gold nanoparticles [47]. Laser ablation efficiency increased when the laser wavelength increasing. It was found that, the optimum ablation laser wavelength was 1064 nm as shown in **Figure 9**. From the above figure, the intensity of surface Plasmon peak of GNPs prepared at 1064 nm is higher than that prepared at 532 nm, which indicated that the amount of GNPs prepared at 1064 nm higher than that prepared at 532 nm.

3.3. Effect of Geometry of Focusing Conditions

In this section two parameters (focal length and the target position) which affect on the shapes and size distribution of obtained GNPs which prepared in pure water are studied. The target position: there are three positions are studied (above focus, at focus and below focus) for a lens has 5 cm focal length. As shown in **Figure 10**, TEM for gold nanoparticles were prepared above focusing

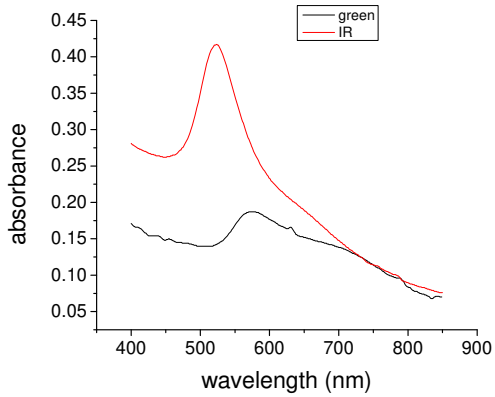

Figure 9. Shows the absorbance spectrum of gold nanoparticles prepared in deionised water at 1064 nm and 532 nm.

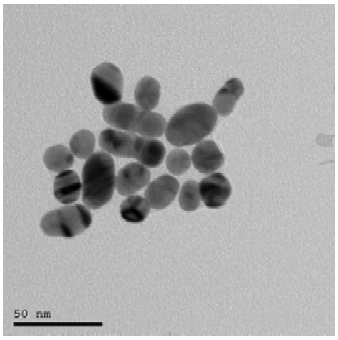

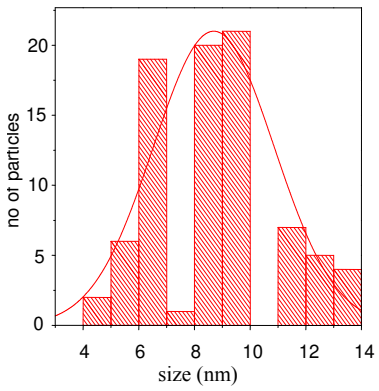

Figure 10. The TEM micrograph and histogram of GNPs prepared in pure water above focusing condition.

conditions.

From **Figure 10**, it's shown that the average size of the obtained particles is 8.6 nm, the yield is small and particles are diffused, this may be due to the low fluence and water breakdown doesn't take place [48], at this fluence the target heated and due to the the strong confinement of the liquid at the surface and the vaporization rate is strongly restricted and no plume forms [49]. **Figure 11** shows GNPs prepared at focusing condition.

As shown from the figure the average particle size is 8.9 nm, which is larger than gold nanoparticles prepared at defocusing condition and the particles have a spherical

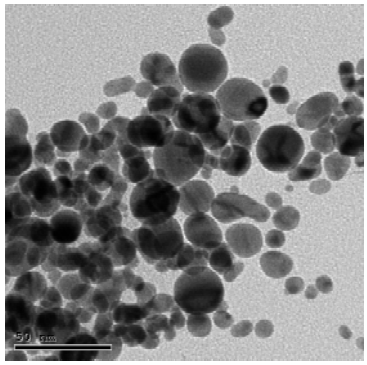

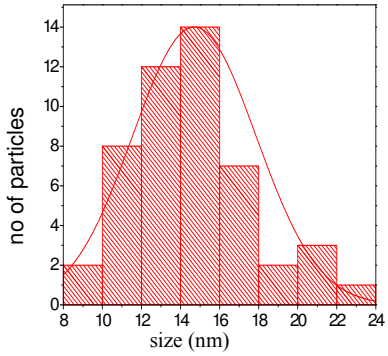

Figure 11. The TEM micrograph and histogram of GNPs prepared in pure water at focusing condition.

shapes and are also agglomerated, this can be explained as, when the ablation takes place at focus the plasma pressure, temperature and density increase more than in the defocusing condition. High temperature of plasma temperature excites, ionizes and dissociates the surrounding water layer, the nucleation starts directly. The high plasma density increases the molecular interaction and particles growth so as a result the particles size increase as observed. When laser is off plasma cooling and recombination take place, pressure and temperature will reduce but particle growth continue until certain value above which it's growth stopped.

When the gold nanoparticles prepared below focusing condition as shown in **Figure 12**, unexpected results obtain as the average size of the obtained particles decreased to 7.2 nm.

In this case the laser irradiation onto the target, most of the energy at the focal region is absorbed by the water, the energy reaches to the target reduces [43], also the liquid increasing the amount of screening of laser light [46] so the energy reached to the target is low and the same results obtained when lens of 10 cm focal length is used as shown in **Table 2**.

Another parameter of the focusing conditions that affect the shape and size distributions of the gold nanoparticles is the lens effect. Since each lens produces a different energy density distribution in space. In each case the sample has been placed at the focus. The minimum

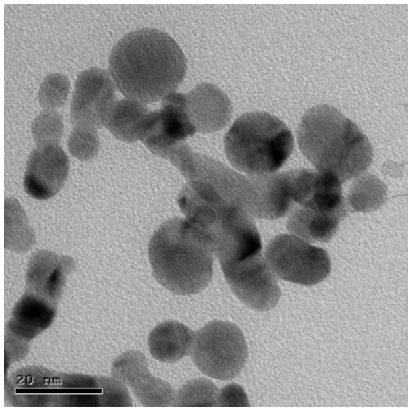

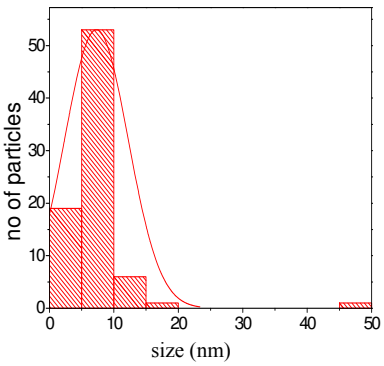

Figure 12. shows the TEM micrograph and histogram for GNPs prepared in pure water below focusing condition.

Table 2. The average size and the particle distribution of GNPs at different focal length and target positions.

	Target position	Average size (nm)	Particle distribution (nm)
f = 5 cm	Above focusing	8	8 - 14
	At focusing	9	15 - 23
	Below focusing	7	9 - 45
f = 10 cm	Above focusing	8	8 - 15
	At focusing	10	10 - 19
	Below focusing	8	6 - 16

diameter of laser beam spot at the focus changes with changing the lens. This in turns changes the laser fluence and hence producing gold nanoparticles with different shapes and sizes. Laser plasma is known to be highly dependent on the laser power density at the surface [40]. **Figures 13(a)-(c)** show TEM and histogram of GNPs prepared by using lenses with different focal length (5, 10, 20 cm), the average size of obtained GNPs are 8.9, 9.8, 17.8 nm respectively.

From the **Figures 14**, **15** and **Table 3**, the laser fluence decrease as the focal length increase as a result the average size increase and the yield of obtained particles also increase. At small focal length (f = 5 cm), very small and hot plasma produced due to high energy density (0.454 MW/m^2) that is localized at the focal point and as a result the average size of produced GNPs is small and have spherical shape and the yield is large and this may be due to the absorption of laser energy in liquid reaches to the target resulting material removing by reactive sputtering [45]. while GNPs prepared at focal length (f = 10 cm), the laser fluence is lower (0.113708 MW/m^2), so the particles obtained are enlarged and the distribution became abroad because the laser pulses producing collides above the sample, the next pulse is partially scattered by these collides particles, so the energy scattered and only too small portion of the energy reached to surface of the target. At focal length (f = 20 cm) the average size of GNPs is larger than that obtained at focal length 5, 10 cm as the laser fluence became smaller (0.028427 MW/m^2) due to the long (tail) along laser beam as the same collides effect and the energy of laser beam is scattered so very small amount of energy is reached to the target resulting in small yield, large average size and broadened distribution.

Figure 16 shows the absorbance spectrum of GNPs prepared at focal length 5, 10, 20 cm, the height of peak decrease with increasing the focal length and that contributed to the small yield obtain as focal length increase also there is a red shift in wavelength with increasing the focal length and that contributed to the increase in the

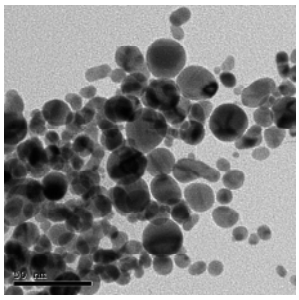

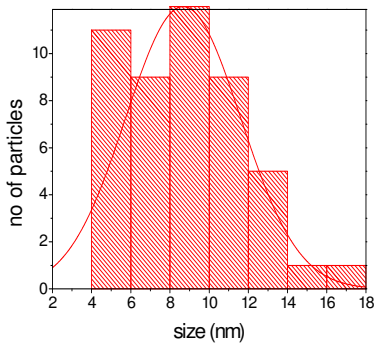

(a)

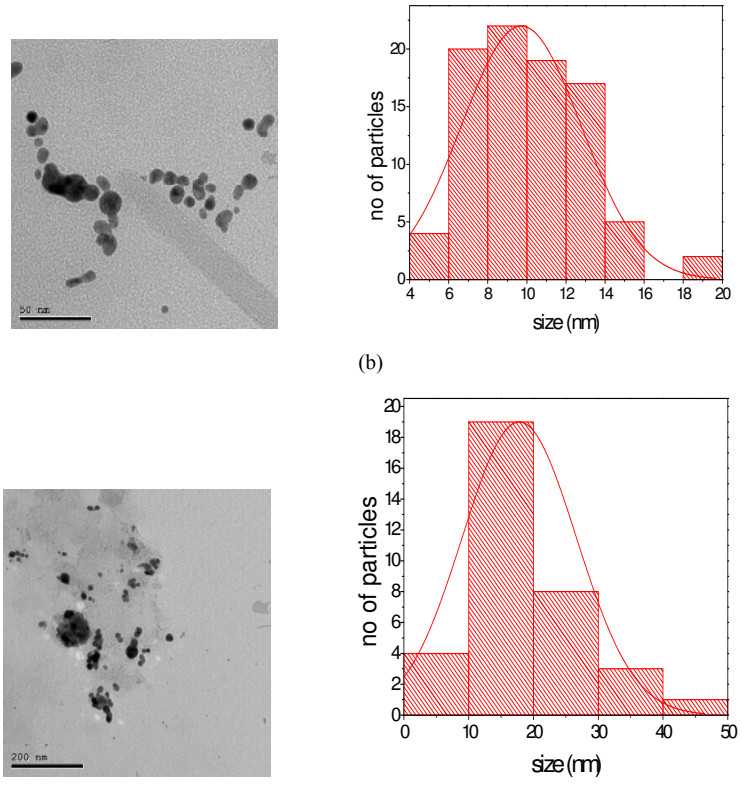

Figures 13. (a)-(c) TEM micrograph and histogram of GNPs prepared in pure water at focal length 5, 10, 20 cm.

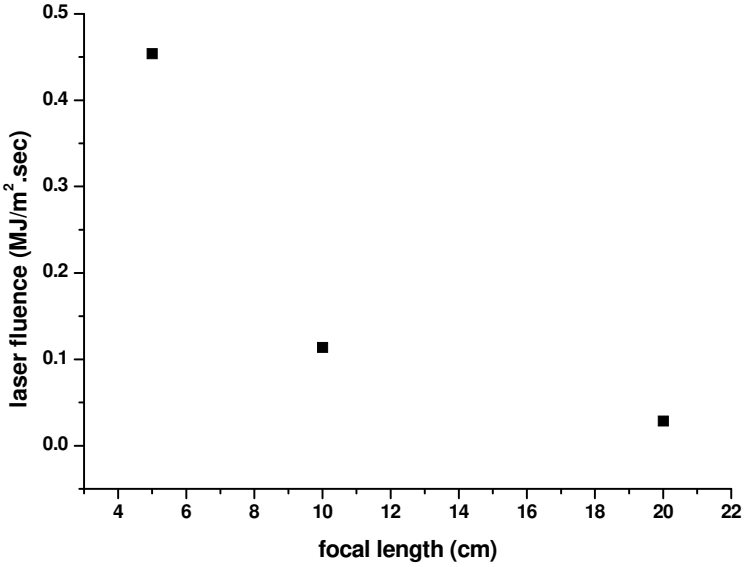

Figure 14. Show the dependence of the focal length on the average size and laser fluence respectively.

Table 3. Show relation between the focal length, laser fluence and the average size.

Average size (nm)	$d_{min} = 2.44\ f\lambda/D$ m	Irradiance (I = P/A) MW/m^2	Focal length (cm)
9	2.16×10^{-6}	0.454	5
10	4.32×10^{-5}	0.113708	10
18	8.6×10^{-5}	0.028427	20

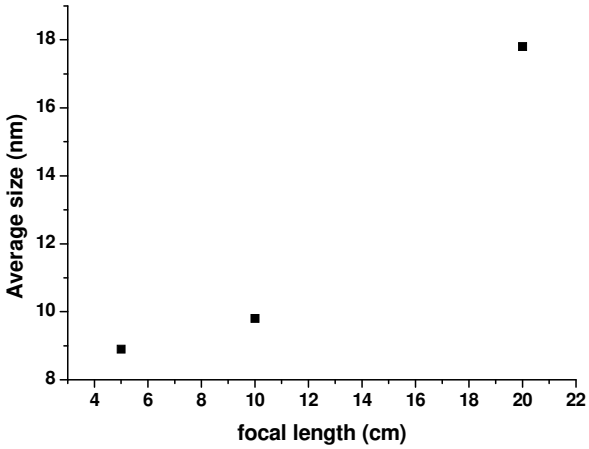

Figure 15. Show the dependence of the focal length on the average size and laser fluence respectively.

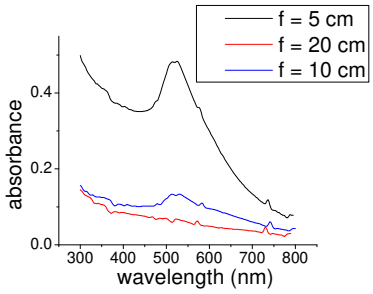

Figure 16. Absorbance spectrum of GNPs prepared at different focal length.

average size of GNPs as focal length increase. That matches with the TEM results.

4. Conclusion

Gold nanoparticles (GNPs) were successively prepared by laser ablation in water. The energy of laser beam affected on the prepared nanoparticles as the energy increases the size of nanoparticles decreases until they reached their critical size below which the particle not sensitive to the laser energy. As the energy increases above this value the nanoparticles begin to agglomerate again and the size increases. Also the wavelength affects the size and yield of the obtained nanoparticles. Smaller size distribution and yield was obtained at shorter wavelength of 532 nm rather than 1064 nm. The focal length and the position of the samples both have a notable affect on the shape and size distribution of the gold nanoparticles. The size distribution and shape can be controlled by optimizing the laser parameter such as energy of laser beam, wavelength or by optimizing the focusing condition of the laser beam.

REFERENCES

[1] F. K. Alanazi, A. A. Radwan and I. A. Alsarra, "Biopharmaceutical Applications of Nanogold," *Saudi Pharmaceutical Journal*, Vol. 18, No. 4, 2010, pp. 179-193.

[2] E. J. Yoo, T. Li, H. G. Park and Y. K. Chang, "Size-Dependent Flocculation Behavior of Colloidal Au Nanoparticles Modified with Various Biomolecules," *Ultramicroscopy*, Vol. 108, No. 1, 2008, pp. 1273-1277.

[3] M. Shakibaie, H. Forootanfar, K. Mollazadeh-Moghadam, Z. Bagherzadeh, N. Nafissi-Varcheh, A. R. Shahverdi and M. A. Faramarzi, "Green Synthesis of Gold Nanoparticles by the Marine Microalga Tetraselmis Suecica," *Biotechnology and Applied Biochemistry*, Vol. 57, No. 2, 2010, pp. 71-75. doi:10.1042/BA20100196

[4] C.-M. Shih, Y.-T. Shieh and Y.-K. Twu, "Preparation of gold Nanopowders and Nanoparticles Using Chitosan Suspensions," *Carbohydrate Polymers*, Vol. 78, No. 2, 2009, pp. 309-315. doi:10.1016/j.carbpol.2009.04.008

[5] K. Kalishwaralal, V. Deepak, S. R. K. Pandian and S. Gurunathan, "Biological Synthesis of Gold Nanocubes from Bacillus Licheniformis," *Bioresource Technology*, Vol. 100, No. 21, 2009, pp. 5356-5358.

[6] K. Kalishwaralal, V. Deepak, S. R. K. Pandian, M, Kottaisamy, S. BarathManiKanth, B. Kartikeyan and S. Gurunathan, "Biosynthesis of Silver and Gold Nanoparticles Using *Brevibacterium casei*," *Colloid and Surface*, *B*: *Biointerfaces*, Vol. 77, No. 2, 2010, pp. 257-262. doi:10.1016/j.colsurfb.2010.02.007

[7] I. Maliszewska, L. Aniszkiewicz and Z. Sadowski, "Biological Synthesis of Gold Nanostructures Using the Extract of *Trichoderma koningii*," *Acta Physica Polonic A*, Vol. 116, 2009, p. S-163.

[8] P. Mukherjee, S. Senapati, D. Mandal, A. Ahmad, M. I. Khan, R. Kumar and M. Sastry, "Extracellular Synthesis of Gold Nanoparticles by the Fungus *Fusarium oxysporum*," *Biochemistry* (*Chemical Biology*), Vol. 3, No. 5, 2002, pp. 461-463. doi:10.1002/1439-7633(20020503)3:5<461::AID-CBIC461>3.0.CO;2-X

[9] Y. Y. Fong, J. R. Gascooke, B. R. Visser, G. F. Metha and M. A. Buntine, "Laser-Based Formation and Properties of Gold Nanoparticles in Aqueous Solution: Formation Kinetics and Surfactant-Modified Particle Size Dis-

tributions," *The Journal of Physical Chemistry C*, Vol. 114, No. 38, 2010, pp. 15931-15940. doi:10.1021/jp9118315

[10] F. Mafuné, J. Y. Kohno, Y. Takeda and T. Kondow, "Growth of Gold Clusters into Nanoparticles in a Solution Following Laser-Induced Fragmentation," *The Journal of Physical Chemistry B*, Vol. 106, No. 34, 2002, pp. 8555-8561.

[11] F. Mafuné, J. Y. Kohno, Y. Takeda and T. Kondow, "Dissociation and Aggregation of Gold Nanoparticles under Laser Irradiation," *The Journal of Physical Chemistry B*, Vol. 105, No. 38, 2001, pp. 9050-9056. doi:10.1021/jp0111620

[12] D. Pissuwan, T. Niidome and M. B. Cortie, "The Forthcoming Applications of Gold Nanoparticles in Drug and Gene Delivery Systems," *Journal of Controlled Release*, Vol. 149, No. 1, 2011, pp. 65-71. doi:10.1016/j.jconrel.2009.12.006

[13] P. Ghosh, G. Han, M. De, C. K. Kim and V. M. Rotello, "Gold Nanoparticles in Delivery Applications," *Advanced Drug Delivery Reviews*, Vol. 60, No. 11, 2008, pp. 1307-1315. doi:10.1016/j.addr.2008.03.016

[14] D. T. Nguyen, D.-J. Kim and K.-S. Kim, "Controlled Synthesis and Biomolecular Probe Application of Gold Nanoparticles," *Micron*, Vol. 42, No. 3, 2011, pp. 207-227. doi:10.1016/j.micron.2010.09.008

[15] A. B. Etame, C. A. Smith, W. C. W. Chan and J. T. Rutka, "Design and Potential Application of PEGylated Gold Nanoparticles with Size-Dependent Permeation through Brain Microvasculature," *Nano Medicine*: *Nanotechnology*, *Biology and Medicine*, Vol. 7, No. 6, 2011, pp. 992-1000. doi:10.1016/j.nano.2011.04.004

[16] T. Donnelly, S. Krishnamurthy, K. Carney, N. McEvoy and J. G. Lunney, "Pulsed Laser Deposition of Nanoparticle Films of Au," *Applied Surface Science*, Vol. 254, No. 4, 2007, pp. 1303-1306. doi:10.1016/j.apsusc.2007.09.033

[17] S. Yang, Y.-H. Jang, C. H. Kim, C. Hwang, J. Lee, S. Chae, S. Jung and M. Choi, "A Flame Metal Combustion Method for Production of Nanoparticles," *Powder Technology*, Vol. 197, No. 3, 2010, pp. 170-176. doi:10.1016/j.powtec.2009.09.011

[18] C. Wu, X. Qiao, J. Chen, H. Wang, F. Tan and S. Li, "A Novel Chemical Route to Prepare ZnO Nanoparticles," *Materials Letters*, Vol. 60, No. 15, 2006, pp. 1828-1832. doi:10.1016/j.matlet.2005.12.046

[19] H. Jia, J. Zeng, W. Song, J. An and B. Zhao, "Preparation of Silver Nanoparticles by Photo-Reduction for Surface-Enhanced Raman Scattering," *Thin Solid Films*, Vol. 496, No. 2, 2006, pp. 281-287. doi:10.1016/j.tsf.2005.08.359

[20] P. Y. Lim, R. S. Liu, P. L. She, C. F. Hung and H. C. Shih, "Synthesis of Ag Nanospheres Particles in Ethylene Glycol by Electrochemical-Assisted Polyol Process," *Chemical Physics Letters*, Vol. 420, No. 4-6, 2006, pp. 304-308. doi:10.1016/j.cplett.2005.12.075

[21] M. J. Rosemary and T. Pradeep, "Solvothermal Synthesis of Silver Nanoparticles from Thiolates," *Journal of Colloid and Interface Science*, Vol. 268, No. 1, 2003, pp. 81-84. doi:10.1016/j.jcis.2003.08.009

[22] M. Szymańska-Chargot, A. Gruszecka, A. Smolira, J. Cytawa and L. Michalak, "Mass-Spectrometric Investigations of the Synthesis of Silver Nanoparticles via Electrolysis," *Vacuum*, Vol. 82, No. 10, 2008, pp. 1088-1093. doi:10.1016/j.vacuum.2008.01.022

[23] H. Huang and X. Yang, "Synthesis of Polysaccharide-Stabilized Gold and Silver Nanoparticles: A Green Method," *Carbohydrate Research*, Vol. 339, No. 15, 2004, pp. 2627-2631. doi:10.1016/j.carres.2004.08.005

[24] J. Gu, W. Fan, A. Shimojima and T. Okubo, "Microwave-Induced Synthesis of Highly Dispersed Gold Nanoparticles within the Pore Channels of Mesoporous Silica," *Journal of Solid State Chemistry*, Vol. 181, No. 4, 2008, pp. 957-963. doi:10.1016/j.jssc.2008.01.039

[25] Y.-C. Liu, L.-H. Lin and W.-H. Chiu, "Size-Controlled Synthesis of Gold Nanoparticles from Bulk Gold Substrates by Sonoelectrochemical Methods," *Journal Physical Chemistry B*, Vol. 108, No. 50, 2004, pp. 19237-19240. doi:10.1021/jp046866z

[26] H. Eerikainen and E. Kauppinen, "Preparation of Polymeric Nanoparticles Containing Corticosteroid by a Novel Aerosol Flow Reactor Method," *International Journal of Pharmaceutics*, Vol. 263, No. 1-2, 2003, pp. 69-83. doi:10.1016/S0378-5173(03)00370-3

[27] K. L. McGilvray, M. R. Decan, D. Wang and J. Scaiano, "Facile Photochemical Synthesis of Unprotected Aqueous Gold Nanoparticles," *Journal of the American Chemical Society*, Vol. 128, No. 50, 2006, pp. 15980-15981. doi:10.1021/ja066522h

[28] M. Duocastella, J. M. Fernandez-Pradas, J. Dominguez, P. Serra and J. L. Morenza, "Printing Biological Solutions through Laser-Induced Forward Transfer," *Applied Physics A*, Vol. 93, No. 4, 2008, pp. 941-945. doi:10.1007/s00339-008-4741-6

[29] Y. Itoh, M. Abdullah and K. Okuyama, "Direct Preparation of Nonagglomerated Indium Tin Oxide Nanoparticles using Various Spray Pyrolysis Methods," *Journal of Materials Research*, Vol. 19, No. 4, 2004, pp. 1077-1086. doi:10.1557/JMR.2004.0141

[30] S. Y. Yang and S. G. Kim, "Characterization of Silver and Silver/Nickel Composite Particles Prepared by Spray Pyrolysis," *Powder Technology*, Vol. 146, No. 3, 2004, pp. 185-192. doi:10.1016/j.powtec.2004.07.010

[31] N. S. Tabrizi, M. Ullmann, V. A. Vons, U. Lafont and A. Schmidt-Ott, "Generation of Nanoparticles by Spark Discharge," *Journal of Nanoparticle Research*, Vol. 11, No. 2, 2009, pp. 315-332. doi:10.1007/s11051-008-9407-y

[32] J.-P. Sylvestre, A. V. Kabashin, E. Sacher, M. Meunier and J. H. T. Luong, "Stabilization and Size Control of Gold Nanoparticles during Laser Ablation in Aqueous Cyclodextrins," *Journal of the American Chemical Society*, Vol. 126, No. 23, 2004, pp. 7176-7177. doi:10.1021/ja048678s

[33] A. Fojtik, A. Henglein and B. Bunsen-Ges, "Laser Ablation of Films and Suspended Particles in Solvent-Formation of Cluster and Colloid Solutions," *Chemical Physics*, Vol. 97,

No. 2, 1993, pp. 252-254.

[34] S. Machmudah, Wahyudiono, Y. K. M. Sasaki and M. Goto, "Nano-Structured Particles Production Using Pulsed Laser Ablation of Gold Plate in Supercritical CO_2," *Journal of Supercritical Fluids*, Vol. 60, 2011, pp. 63-68. doi:10.1016/j.supflu.2011.04.008

[35] N. V. Tarasenko, A. V. Butsen, E. A. Nevar and N. A. Savastenko, "Synthesis of Nanosized Particles during Laser Ablation of Gold in Water," *Applied Surface Science*, Vol. 252, No. 13, 2006, pp. 4439-4444. doi:10.1016/j.apsusc.2005.07.150

[36] H. J. Kim, I. C. Bang and J. Onoe, "Characteristic Stability of Bare Au-Water Nanofluids Fabricated by Pulsed Laser Ablation in Liquids," *Optics and Laser in Engineering*, Vol. 47, No. 5, 2009, pp. 535-538. doi:10.1016/j.optlaseng.2008.10.011

[37] S. I. Dolgaev, A. V. Simakin, V. V. Voronov, G. A. Shafeev and F. B. Verduraz, "Nanoparticles Produced by Laser Ablation of Solids in Liquid Environment," *Applied Surface Science*, Vol. 186, No. 1-4, 2002, pp. 546-551. doi:10.1016/S0169-4332(01)00634-1

[38] N. Haustrup and G. M. Oconnor, "Nanoparticle Generation during Laser Ablation and Laser-Induced Liquefaction," *Physics Procedia*, Vol. 12, Part B, 2011, pp. 53-64.

[39] T. Sakai, H. Enomoto, K. Torigoe, H. Sakai and M. Abe, "Surfactant- and Reducer-Free Synthesis of Gold Nanoparticles in Aqueous Solutions," *Colloids and Surfaces A*: *Physicochemical and Engineering Aspects*, Vol. 347, No. 1-3, 2008, pp. 18-26. doi:10.1016/j.colsurfa.2008.10.037

[40] P. Calandra, C. Giordano, A. Longo and V. TurcoLireri, "Physicochemical Investigation of Surfactant-Coated Gold Nanoparticles Synthesized in the Confined Space of Dry Reversed Micelles," *Materials Chemistry and Physics*, Vol. 98, No. 2-3, 2006, pp. 494-499. doi:10.1016/j.matchemphys.2005.09.068

[41] F. K. Liu, "Extremely Highly Efficient On-Line Concentration and Separation of Gold Nanoparticles Using the Reversed Electrode Polarity Stacking Mode and Surfactant-Modified Capillary Electrophoresis," *Analytica Chimica Acta*, Vol. 694, No. 1-2, 2011, pp. 167-173. doi:10.1016/j.aca.2011.03.056

[42] J. P. Sylvestre, S. Poulin, E. Sacher, M. Meunier and J. H. T. Luong, "Surface Chemistry of Gold Nanoparticles Produced by Laser Ablation in Aqueous Media," *Journal of Physical Chemistry B*, Vol. 108, No. 34, 2004, pp. 16864-16869. doi:10.1021/jp047134+

[43] B. Xu, R. G. Song, P. H. Tang, J. Wang, G. Z. Chai, Y. Z. Zhang and Z. Z. Ye, "Preparation of Ag Nanoparticles Colloid by Pulsed Laser Ablation in Distilled Water," *Key Engineering Materials*, Vol. 373-374, 2008, pp. 346-349.

[44] A. Sasoh, K. Watanabe, Y. Sano and N. Mukai, "Behavior of Bubbles Induced by the Interaction of a Laser Pulse with a Metal Plate in Water," *Applied Physics A*: *Material Science & Processing*, Vol. 80, No. 7, 2005, pp. 1497-1500.

[45] W. T. Nichols, T. Sasaki and Naoto Koshizaki, "Laser Ablation of a Platinum Target in Water. I. Ablation Mechanisms," *Journal of Applied Physics*, Vol. 100, No. 11, 2006, pp. 114911-114917. doi:10.1063/1.2390640

[46] W. T. Nichols, T. Sasaki and N. Koshizaki, "Laser Ablation of a Platinum Target in Water. III. Laser-Induced Reactions," *Journal of Applied Physics*, Vol. 100, No. 11, pp. 112006-114913. doi:10.1063/1.2390642

[47] P. Smejkal, J. Pfleger, B. Vlckova and O. Dammer, "Laser Ablation of Silver in Aqueous Ambient: Effect of Laser Pulse Wavelength and Energy on Efficiency of the Process," *Journal of Physics: Conferences Series*, Vol. 59, 2007, p. 185.

[48] A. Natha, S. S. Lahaa and A. Khare, "Effect of Focusing Conditions on Synthesis of Titanium Oxide Nanoparticles Via Laser Ablation in Titanium-Water Interface," *Applied Surface Science*, Vol. 257, No. 7, 2011, p. 3118.

[49] V. Bulatov, L. Xu and I. Schechter, "Spectroscopic Imaging of Laser-Induced Plasma," *Analytical Chemistry*, Vol. 68, No. 17, 1996, pp. 2966-2973. doi:10.1021/ac960277a

